

Crystal Structure and Magnetic Properties of the Quasi-One-Dimensional Quantum Spin System $\text{Cu}_2\text{Cl}_4\cdot\text{H}_8\text{C}_4\text{SO}_2$

Masashi FUJISAWA*, Jun-Ichi YAMAURA¹, Hidekazu TANAKA², Hiroshi KAGEYAMA¹,
Yasuo NARUMI^{3,4} and Koichi KINDO^{3,4}

Department of Physics, Tokyo Institute of Technology, Oh-okayama, Meguro-ku, Tokyo 152-8551

¹*Institute for Solid State Physics, The University of Tokyo, Kashiwanoha, Kashiwa, Chiba 277-8581*

²*Research Center for Low Temperature Physics, Tokyo Institute of Technology, Meguro-ku, Tokyo 152-8551*

³*CREST, Japan Science and Technology, Kawaguchi, Saitama 332-0012*

⁴*Research Center for Materials Science at Extreme Conditions, Osaka University, Toyonaka, Osaka 560-0043*

(Received October 2, 2002)

The crystal structure of $\text{Cu}_2\text{Cl}_4\cdot\text{H}_8\text{C}_4\text{SO}_2$ was analyzed by single-crystal X-ray diffraction. This compound consists of the double chain of the edge-sharing octahedra CuCl_5O . With decreasing temperature, the magnetic susceptibility decreases steeply toward zero below 10 K after exhibiting a broad maximum at 65 K, which is characteristic of the one-dimensional antiferromagnet. The magnetic properties of the present system can be described by the double spin chain model with dominant exchange interactions along the leg. The observed small excitation gap $\Delta/k_B \approx 5.8$ K is attributed to the weak exchange alternation along the leg or the weak zig-zag rung interactions. The magnetization curve measured at 1.3 K for the magnetic field parallel to the c -axis shows a discontinuous jump at $H_t \approx 22.8$ T indicative of the phase transition of the first order.

KEYWORDS: $\text{Cu}_2\text{Cl}_4\cdot\text{H}_8\text{C}_4\text{SO}_2$, crystal structure, double chain, singlet ground state, excitation gap, bond alternation, magnetic susceptibility, high-field magnetization process, ESR

DOI: 10.1143/JPSJ.72.694

1. Introduction

The crystal structure of $\text{Cu}_3\text{Cl}_6(\text{H}_2\text{O})_2\cdot 2\text{H}_8\text{C}_4\text{SO}_2$ was reported by Swank and Willet.¹⁾ The crystal structure has an infinite chain composed of Cu_3Cl_6 trimers. Ishii *et al.*²⁾ presented the magnetic properties of $\text{Cu}_3\text{Cl}_6(\text{H}_2\text{O})_2\cdot 2\text{H}_8\text{C}_4\text{SO}_2$. The compound has a singlet ground state with a small excitation gap $\Delta/k_B \approx 5.2$ K. They interpreted the gapped ground state in terms of a trimer chain model. However, the temperature dependence of the magnetic susceptibilities and the angular dependence of the g -factor observed could not be understood in terms of the trimer chain model³⁾ and the crystal structure, respectively. Thus, we re-examined the crystal structure by X-ray diffraction using single crystals. It was found that the compound assumed to be $\text{Cu}_3\text{Cl}_6(\text{H}_2\text{O})_2\cdot 2\text{H}_8\text{C}_4\text{SO}_2$ by Ishii *et al.*²⁾ was actually $\text{Cu}_2\text{Cl}_4\cdot\text{H}_8\text{C}_4\text{SO}_2$. $\text{Cu}_2\text{Cl}_4\cdot\text{H}_8\text{C}_4\text{SO}_2$ is a new compound that has not been reported to date. In this paper, we report its crystal structure and magnetic properties studied by X-ray diffraction, magnetization and ESR measurements.

2. Experimental Procedures

Single crystals of $\text{Cu}_2\text{Cl}_4\cdot\text{H}_8\text{C}_4\text{SO}_2$ were prepared by dissolving CuCl_2 and $\text{H}_8\text{C}_4\text{SO}_2$ in ethyl alcohol. The solution was evaporated at 60°C over six weeks. Long platelet crystals were obtained.

In the X-ray crystal structure analysis, the intensity data were collected using an imaging plate type Weissenberg camera (Mac Science DIP 320 V) with graphite monochromated $\text{Mo K}\alpha$ radiation ($2\theta < 60^\circ$). Absorption and decay were corrected in the data merging process. The structure was solved by the direct method⁴⁾ and refined by the full-matrix least-squares method using *teXsan* program package.

Table I. Crystal data for $\text{Cu}_2\text{Cl}_4\cdot\text{H}_8\text{C}_4\text{SO}_2$.

Chemical formula	$\text{Cu}_2\text{Cl}_4\cdot\text{H}_8\text{C}_4\text{SO}_2$
Space group	$P\bar{1}$
a (Å)	9.425(1)
b (Å)	10.793(2)
c (Å)	6.620(1)
α (deg)	98.869(8)
β (deg)	95.25(2)
γ (deg)	120.850(7)
V (Å ³)	559.6(2)
Z	2
No. of observed reflections	1277 ($I > 3\sigma(I)$)
$R; wR$	0.079; 0.121

The crystal data are listed in Table I. The chemical formula was found to be $\text{Cu}_2\text{Cl}_4\cdot\text{H}_8\text{C}_4\text{SO}_2$ from the results of structural and chemical analyses. Since the crystal is very hygroscopic, the surface of the crystal was gradually damaged during the X-ray measurement, which gives rise to the somewhat large R -factor (= 0.079). However, the value of the R -factor is sufficient to show that the structure is correctly solved, although some modification of the atomic parameters will be needed.

The susceptibilities were measured using a SQUID magnetometer (Quantum Design MPMS XL). Since the crystals were highly hygroscopic, we treated them in a glove box filled with dry nitrogen. High-field magnetization measurement was performed using an induction method with a multilayer pulse magnet, at the Research Center for Materials Science at Extreme Conditions, Osaka University. A magnetic field was applied along the long axis c . The magnetization data were collected at 1.3 K in magnetic fields of up to 68 T. ESR spectrum was measured at room temperature using X (~ 9 GHz) band frequency.

*E-mail: mercy@lee.phys.titech.ac.jp.

3. Results and Discussion

3.1 Crystal structure

The atomic parameters are listed in Table II. Figure 1(a) shows the crystal structure of $\text{Cu}_2\text{Cl}_4 \cdot \text{H}_8\text{C}_4\text{SO}_2$. This

Table II. Fractional atomic coordinates and equivalent isotropic displacement parameters (\AA^2). Hydrogen atoms are omitted because we adopt the calculated positions for them.

Atom	<i>x</i>	<i>y</i>	<i>z</i>	U_{eq}
Cu(1)	0.0824(1)	0.37333(10)	0.8518(2)	0.0277(4)
Cu(2)	0.0780(1)	0.3725(1)	0.3523(2)	0.0287(5)
Cl(1)	0.2772(3)	0.4513(2)	1.1483(4)	0.0333(7)
Cl(2)	-0.1159(3)	0.3163(2)	0.5644(4)	0.0305(7)
Cl(3)	0.2776(3)	0.4555(2)	0.6442(4)	0.0335(7)
Cl(4)	-0.1148(3)	0.3153(2)	0.0597(4)	0.0297(7)
S(1)	0.1287(3)	0.0459(2)	-0.2225(3)	0.0350(7)
O(1)	0.0549(9)	0.1349(6)	-0.2149(10)	0.036(2)
O(2)	0.0061(9)	-0.1123(6)	-0.279(1)	0.040(2)
C(1)	0.273(1)	0.096(1)	0.017(2)	0.047(3)
C(2)	0.439(2)	0.176(2)	-0.029(2)	0.096(6)
C(3)	0.433(2)	0.109(1)	-0.261(2)	0.068(4)
C(4)	0.280(2)	0.095(1)	-0.385(2)	0.054(4)

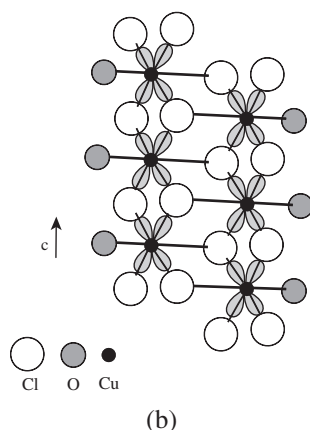
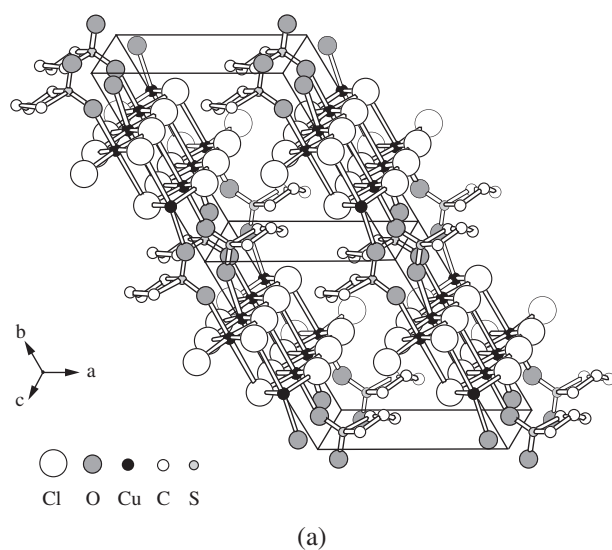


Fig. 1. (a) Crystal structure of $\text{Cu}_2\text{Cl}_4 \cdot \text{H}_8\text{C}_4\text{SO}_2$. (b) Double chain structure composed of edge-sharing CuCl_5O octahedra and the hole orbitals $d(x^2 - y^2)$ of Cu^{2+} ions.

compound is composed of the infinite Cu double chain and the $\text{H}_8\text{C}_4\text{SO}_2$ molecule with short $\text{Cu} \cdots \text{O}$ contacts between them. Figure 1(b) shows a schematic Cu double chain, where the magnetic Cu^{2+} ion is surrounded octahedrally by five chlorine ions and an oxygen atom of $\text{H}_8\text{C}_4\text{SO}_2$. The CuCl_5O octahedra are elongated along the $\text{Cl}'(4)\text{--Cu}(1)\text{--O}(1)$ and $\text{Cl}'(2)\text{--Cu}(2)\text{--O}(2)$ axes which are perpendicular to the chain and parallel to the *b*-axis. The elongation should be ascribed to the Jahn–Teller effect. In one chain of the double chain, the distance between Cu^{2+} ions is slightly alternating, i.e., one is 3.302(2) \AA and the other is 3.318(2) \AA . Therefore, the exchange interactions should be weakly alternating along the chain.

The long direction of the obtained single crystals is the *c* direction. The crystals are easily cleaved along a plane including the *c*-axis. The *g*-factor was measured by ESR. The maximum *g*-factor was obtained when the magnetic field is parallel to the cleavage plane and perpendicular to the *c*-axis. The *g*-factor becomes a maximum when the magnetic field is parallel to the elongated axis of the CuCl_5O octahedron. Thus, the cleavage plane was deduced to be (1,0,0). The *g*-factors for $H \parallel a^*$, *b* and *c*-axes were determined as $g_{a^*} = 2.03$, $g_b = 2.24$ and $g_c = 2.03$, respectively. These field directions are almost perpendicular to one another. The angular dependence of the *g* factor is compatible with the crystal structure determined in the present work.

3.2 Magnetic Properties

The magnetic susceptibilities for $H \parallel a^*$, *b* and *c*-axes are shown in Fig. 2 as a function of temperature. The susceptibilities exhibit the same temperature dependence. The difference between the absolute values of the three susceptibilities is due to the anisotropy of the *g*-factor, because the three susceptibilities almost coincide with one another when normalized by the *g*-factor. The susceptibilities have a broad maximum at around 65 K, which is characteristic of the antiferromagnetic Heisenberg chain. Below 10 K, the susceptibility decreases rapidly toward zero with decreasing temperature. This result indicates that the ground state is a spin singlet with a small excitation gap. Since no anomaly

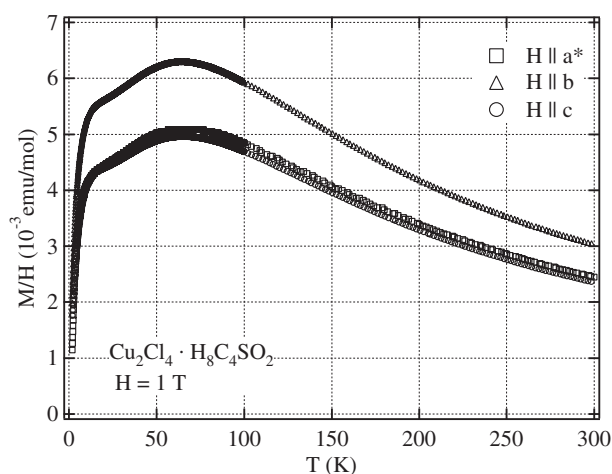


Fig. 2. Temperature dependence of magnetic susceptibilities in $\text{Cu}_2\text{Cl}_4 \cdot \text{H}_8\text{C}_4\text{SO}_2$ measured at $H = 1 \text{ T}$ for $H \parallel a^*$, *b* and *c*-axes.

indicative of the phase transition such as spin–Peierls transition is seen in the susceptibility data, the rapid decrease of the susceptibility is attributed to the crossover from the thermally induced magnetic state to the gapped ground state.

From the crystal structure of $\text{Cu}_2\text{Cl}_4 \cdot \text{H}_8\text{C}_4\text{SO}_2$, we can expect that the hole orbitals $d(x^2 - y^2)$ lie in a plane including the c -axis, and are linked together along the chain, as shown in Fig. 1(b). The configuration of the hole orbitals is similar to that in CuCl_2 ,⁵⁾ which displays magnetic susceptibility typical of the $S = 1/2$ one-dimensional (1D) Heisenberg antiferromagnet.⁶⁾ For CuCl_2 , the broad susceptibility maximum is observed at around 70 K. $\text{Cu}_2\text{Cl}_4 \cdot \text{H}_8\text{C}_4\text{SO}_2$ exhibits almost the same magnetic susceptibility as that of CuCl_2 above 30 K. This susceptibility behavior is consistent with the crystal structure. Below 30 K, the susceptibilities of $\text{Cu}_2\text{Cl}_4 \cdot \text{H}_8\text{C}_4\text{SO}_2$ and CuCl_2 behave differently. The latter undergoes magnetic ordering at $T_N \approx 24$ K.⁷⁾

The exchange interactions in the double chain are thought to be described as shown in Fig. 3. Since the hole orbitals $d(x^2 - y^2)$ are linked together along the chain, the exchange interactions J and J' along the leg of the double chain should be dominant. This can be confirmed from that the present system exhibits magnetic susceptibility typical of the $S = 1/2$ 1D antiferromagnet above 30 K. Since the distance between Cu^{2+} ions along a leg is slightly alternating, $J \neq J'$, although they should be very close to each other. Thus, we compare first the experimental susceptibility with that calculated for the $S = 1/2$ alternating Heisenberg chain.⁸⁾ Experimental and calculated susceptibilities for $H \parallel b$ are plotted in Fig. 4, where α is the alternation parameter

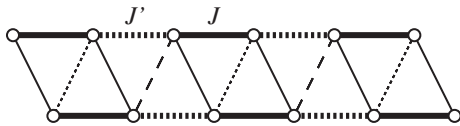


Fig. 3. Exchange interactions in the double chain. Thick solid and dashed lines denote the strong interactions along the leg and thin solid, dashed and dotted lines denote weak zig-zag rung interactions.

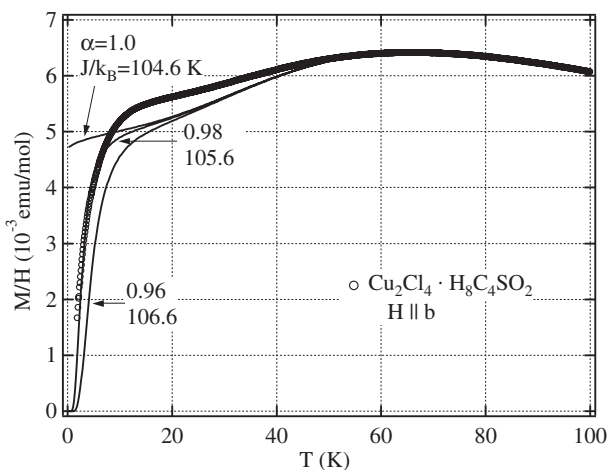


Fig. 4. Observed and calculated magnetic susceptibilities for $H \parallel b$ as functions of temperature. Solid lines denote the results of calculations based on the alternating chain model.

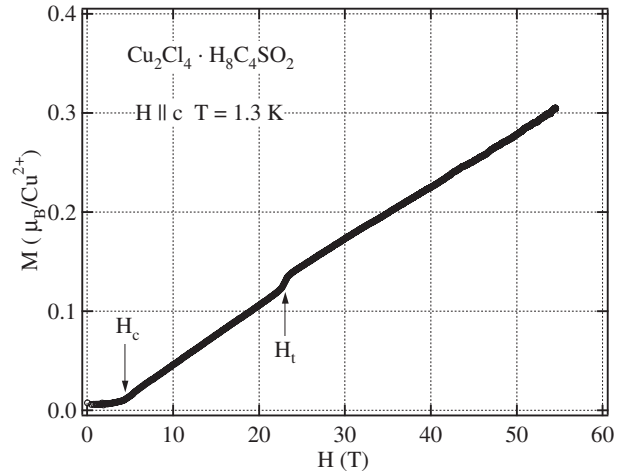


Fig. 5. Magnetization curve for $H \parallel c$ measured at 1.3 K.

defined by $\alpha = J'/J$, and the exchange constants are defined as $\mathcal{H} = \sum_{(i,j)} J_{ij}(\mathbf{S}_i \cdot \mathbf{S}_j)$. The susceptibility calculated with $\alpha = 0.98$ and $J/k_B = 105.6$ K is close to the experimental one. However, there is a significant difference between the experimental and calculated susceptibilities below 50 K.

For the $S = 1/2$ antiferromagnetic spin ladder, it is known that the rung interaction can produce the excitation gap, no matter how small it may be. Thus, there is a possibility that the small excitation gap in $\text{Cu}_2\text{Cl}_4 \cdot \text{H}_8\text{C}_4\text{SO}_2$ arises from the weak zig-zag rung interactions denoted by thin solid, dotted and dashed lines in Fig. 3. The gapped ground state in the present system should be attributed to the exchange alternation along the leg and the zig-zag rung interactions. To the best of the authors' knowledge, the spin model shown in Fig. 3 has not been studied theoretically.

Figure 5 shows the magnetization curve measured at 1.3 K in magnetic fields of up to 54 T for $H \parallel c$. A phase transition is observed at $H_c \approx 4.3$ T, where the excitation gap closes. The ground state becomes gapless for $H > H_c$. From the value of H_c , the magnitude of the gap Δ is evaluated as $\Delta/k_B = g_c \mu_B H_c / k_B \approx 5.8$ K with $g_c = 2.03$ obtained by ESR measurement.

Another phase transition with a small magnetization jump can be observed at $H_t \approx 22.8$ T. The magnitude of the magnetization jump ΔM at H_t is $\Delta M = 0.011 \mu_B$. The phase transition is considered to be of the first order. At present, the mechanism leading to the field-induced phase transition is unknown. We also measured magnetization in magnetic fields of up to 68 T. No anomaly indicative of the additional phase transition was observed above H_t .

4. Conclusion

The new spin gap system reported by Ishii *et al.*²⁾ was found to be $\text{Cu}_2\text{Cl}_4 \cdot \text{H}_8\text{C}_4\text{SO}_2$ and not $\text{Cu}_3\text{Cl}_6(\text{H}_2\text{O})_2 \cdot 2\text{H}_8\text{C}_4\text{SO}_2$. We determined the crystal structure of $\text{Cu}_2\text{Cl}_4 \cdot \text{H}_8\text{C}_4\text{SO}_2$ and investigated its magnetic properties. The present system can be described magnetically by the double spin chain model shown in Fig. 3 with the strong exchange interactions J and J' along the leg. The temperature dependence of the magnetic susceptibility and the angular dependence of the g -factor are compatible with the crystal structure. The ground state of $\text{Cu}_2\text{Cl}_4 \cdot \text{H}_8\text{C}_4\text{SO}_2$ is the spin singlet with the excitation gap $\Delta/k_B \approx 5.8$ K. The

origin of the small gap should be attributed to the weak exchange alternation along the leg or the zig-zag rung interactions. The magnetization curve measured at 1.3 K for the magnetic field parallel to the *c*-axis shows a discontinuous jump at $H_t \approx 22.8$ T indicative of the first order phase transition.

Acknowledgements

The authors would like to thank T. Tonegawa, K. Okamoto, K. Takano and A. Honecker for stimulating discussions. This work was supported by Toray Science Foundation and a Grant-in-Aid for Scientific Research on Priority Areas (B) from the Ministry of Education, Culture, Sports, Science and Technology of Japan.

- 1) D. D. Swank and R. D. Willett: *Inorg. Chim. Acta* **8** (1974) 143.
- 2) M. Ishii, H. Tanaka, M. Hori, H. Uekusa, Y. Ohashi, K. Tatani, Y. Narumi and K. Kindo: *J. Phys. Soc. Jpn.* **69** (2000) 340.
- 3) A. Honecker and A. Läuchi: *Phys. Rev. B* **63** (2001) 174407.
- 4) SIR97 (Program for direct method), A. Altomare, M. C. Burla, M. Camalli, G. L. Cascarano, C. Giacovazzo, A. Guagliardi, A. G. G. Moliterni, G. Polidori and R. Spagna: *J. Appl. Cryst.* **32** (1999) 115.
- 5) A. F. Wells: *J. Chem. Soc.* (1947) 1670.
- 6) D. Billerey, C. Terrier, R. Mainard, M. Permin and J. Hubsch: *Phys. Lett. A* **68** (1978) 275.
- 7) J. W. Stout and R. C. Chisholm: *J. Chem. Phys.* **36** (1962) 979.
- 8) D. C. Johnston, R. K. Kremer, M. Troyer, X. Wang, A. Klümper, S. L. Bud'ko, A. F. Panchula and P. C. Canfield: *Phys. Rev. B* **61** (2000) 9558.